

# RSC Advances



This is an *Accepted Manuscript*, which has been through the Royal Society of Chemistry peer review process and has been accepted for publication.

*Accepted Manuscripts* are published online shortly after acceptance, before technical editing, formatting and proof reading. Using this free service, authors can make their results available to the community, in citable form, before we publish the edited article. This *Accepted Manuscript* will be replaced by the edited, formatted and paginated article as soon as this is available.

You can find more information about *Accepted Manuscripts* in the [Information for Authors](#).

Please note that technical editing may introduce minor changes to the text and/or graphics, which may alter content. The journal's standard [Terms & Conditions](#) and the [Ethical guidelines](#) still apply. In no event shall the Royal Society of Chemistry be held responsible for any errors or omissions in this *Accepted Manuscript* or any consequences arising from the use of any information it contains.

**Environmentally benign bio-inspired synthesis of Au nanoparticles, their self-assembly and agglomeration**

Ramesh Raliya and Pratim Biswas\*

Aerosol and Air Quality Research Laboratory,  
Dept. of Energy, Environmental and Chemical Engineering  
Washington University in St. Louis  
St. Louis, MO 63130, USA

**Revised Manuscript Submitted to**

**RSC Advances**

*Article History*

**First submission:** March 15, 2015

**Revised Manuscript Submitted:** April 18, 2015

**\*Corresponding author**

Email: [pbiswas@wustl.edu](mailto:pbiswas@wustl.edu)

Phone: +1 (314) 935-5482

## **Benign bio-inspired synthesis of Au nanoparticles, their self-assembly and agglomeration**

The synthesis and characterization of stable gold nanoparticles (AuNPs) from gold chloride in soluble protein extracts of tomato (*Solanum lycopersicum* L) leaves is demonstrated. This approach is a completely “green” synthetic method, which is simple, environmentally benign, and efficient, in contrast to conventional approaches that use toxic or hazardous chemicals, high temperature, pressure, and pH. As observed by transmission electron microscopy, the as synthesized nanoparticles were spherical and 13-15 nm diameter. The agglomeration and electro-kinetic properties of the biologically reduced Au NPs were also studied. Au NPs with thiol and amino groups was successfully functionalized which was confirmed by investigation of Au NP self-assembly in the presence of L-cysteine.

## 1. Introduction

Gold nanoparticles (Au NPs) are one of the most stable metal nanoparticles,<sup>1</sup> and they have novel characteristics, such as assembly to form multiple structures; size-related electronic, magnetic, and optical properties (quantum size effect); and applications in catalysis and biology.<sup>2-4</sup> Au NPs, can be prepared by both physical and chemical approaches.<sup>5-8</sup> Most chemical approaches use some toxic substances, such as reducing agents (sodium borohydrate) and capping agents (cetyl tri-methyl ammonium bromide/chloride) during the process of particle formation and stabilization. Physical approaches are much more expensive and have low rates of particle formation. These drawbacks have led researchers to further investigate economically viable and environmentally benign (green) approaches for Au NP synthesis.

A green approach is a method which uses or produces non-toxic and environmentally sustainable materials. These methods are preferred over conventional approaches because of advantages including safer design, reduced environmental impact, waste reduction, process safety, and improved material and environmental efficiency.<sup>9, 10</sup> To advance green nanotechnology, several attempts have been made to synthesize Au NPs by using microbes, including fungi, bacteria and actinomycetes.<sup>11-18</sup> In recent years, the development of efficient green chemistry methods for the synthesis of noble metal nanoparticles has become a major research focus in improving the biogenic process. Specifically, attempts have been made using plant extracts. Basavegowda et al.,<sup>19</sup> described the room temperature synthesis of ~20 nm Au NPs using an aqueous extract of *Hovenia dulcis* fruit. Similarly, Zayed and Eisa<sup>20</sup> synthesized AuNP (32-45 nm) to explore the reducing and capping potential of the *Phoenix dactylifera* extract for catalytic activity. In comparison to microbes, plants seem to be the best candidates,

for large-scale biosynthesis of nanoparticles. Nanoparticles produced by plants are more stable, and their rate of synthesis is faster than that of microorganisms.<sup>21</sup>

To identify the best candidates for fine metal nanoparticle production, researchers have focused on plants with high potential for heavy metal accumulation. One such plant, tomato (*Solanum lycopersicum* L) is grown worldwide for its edible fruit with nutritional importance. Typically, after the fruits are picked, the remaining biomass is discarded. However, the tomato plant leaf has abundant antioxidant enzymes that may serve as reducing agents for precursor metal salts. Bio-reduction is a promising pathway of the potential scaled-up production of metal nanoparticles. According to the available literature, one group,<sup>22</sup> reports Au NP synthesis from red tomato fruit, in which Au NPs are fabricated using aqueous extract of red tomato. The importance of the tomato plant for the large scale synthesis of Au NPs is relatively unexplored. In this work, tomato leaf biomass for Au NPs synthesis is demonstrated. To the best of our knowledge there is no published report for Au NP synthesis using tomato plant leaf extracts.

Ionic substances and organic solvents affect nanoparticle transport behavior.<sup>23, 24</sup> Common monovalent and divalent ionic substances such as NaCl, CaCl<sub>2</sub> and MgCl<sub>2</sub>, and ethanol are used to investigate Au NP agglomeration properties. Furthermore, aqueous environments also affect electro-kinetic properties of nanoparticles. To utilize NPs for biomedical applications, NPs must be functionalized for cellular transport and target site internalization.<sup>25</sup> Functionalization with amino (-NH<sub>2</sub>) and thiol (-SH) group are common. L-cysteine, which contains both amino -NH<sub>2</sub> and -SH groups, was used to test functionalization, and its effect on the self-assembly of Au NPs.

The present paper reports a synthesis method for Au NPs that eliminates the need for harmful reagents and results in no waste byproducts, while enhancing the synthesis efficiency in

comparison to other biological synthesis approaches that use microbes and tissue lysate. The agglomeration behavior in an aqueous environment of electrolytes and ethanol under varying concentrations with time is studied. In addition, self-assembly due to  $-NH_2$  and  $-SH$  group was tested for functionalization. This report is novel in describing Au NP synthesis from tomato leaves,  $-NH_2$  and  $-SH$  functionalization, and the exploration of its agglomeration properties in different salt and ethanol concentrations.

## 2. Experimental

The experimental plan is summarized in **Table 1**. The primary objective was to synthesize Au NPs, and secondary objectives were to study their agglomeration and functionalization; and an experimental plan is described in the following sections.

### 2.1. Green synthesis of Au NPs and their characterization

A schematic process diagram for Au NPs synthesis is described in **Figure 1**, and the following sections outline the various steps.

#### 2.1.1. Isolation and quantification of plant protein

Fresh leaves of 14 day old tomato plants (*Lycopersicon esculentum* L) were collected and 1gm was homogenized in 10 mL of 10% tri-chloro acetic acid (TCA) in cold acetone. The homogenate was kept in a refrigerator at  $-2^\circ\text{C}$  for 1h to precipitate proteins and extract leaf pigments. Subsequently, the mixture was centrifuged for 10 min. at  $10^4$  g and  $4^\circ\text{C}$  to halt enzymatic activities. This process was repeated three times to precipitate the proteins and completely remove plant pigments. The obtained pellet was re-suspend in cold deionized (DI) water and centrifuged for 10 min. at 6000g and  $4^\circ\text{C}$ . The resultant supernatant containing soluble protein was used for the synthesis of Au NPs.

To optimize the Au NP synthesis process, it is important to know the protein concentration, and this was quantified by following the Lowry method (Lowry et al., 1951). In brief, samples were pretreated with copper ion in an alkali solution. In this treatment, aromatic amino acids of the treated sample reduce the phosphor-molybdate-phospho-tungstic acid present in Folin reagent, leading to the formation of a blue color complex. The intensity is measured by a spectrophotometer at 750 nm.

### **2.1.2. NPs synthesis: time dependent investigation**

Au NPs were synthesized using soluble plant proteins and a precursor salt, gold (III) chloride trihydrate ( $\text{HAuCl}_4 \cdot 3\text{H}_2\text{O}$ ). To synthesize Au NPs, protein and precursor salt were mixed at a 1:1 ratio at room temperature ( $22^\circ\text{C} \pm 2$ ) under a static condition. The solution mixture was kept in the dark (to avoid degradation by photo-thermal effect) for 72 h. In the meantime, UV-Vis absorption was recorded with different time intervals (0, 6, 12, 18, 24 and 36h) to assess the formation of Au NPs.

### **2.1.3. Effect of protein concentration on Au NPs formation**

Enzyme activity depends on pH, temperature, and ionic strength. In addition, the rate of enzyme-mediated reactions depends on the number of active sites available to carry out the reaction. Thus, the formation of Au NPs was studied using varying protein content. In our experimental design, varying amounts of the protein solution from 100  $\mu\text{L}$  to 1000  $\mu\text{L}$  were diluted with DI water for a total volume of 1 mL. In the protein solution, 100  $\mu\text{L}$  of precursor salt (4.86 mM,  $\text{HAuCl}_4 \cdot 3\text{H}_2\text{O}$ ) was added, and the mixture was incubated for 36 h at room temperature. After incubation, the synthesized NPs were characterized by UV-Vis absorption spectra.

#### 2.1.4. Purification of synthesized Au NPs

To purify NPs from plant proteins for further study, a 10% TCA was used to precipitate the plant proteins, followed by centrifugation at  $10^4$  g for 15 min. NPs were triple washed using centrifugation and re-suspending the pellet of NPs with TCA. Finally, Au NPs were dispersed in DI water, and used for further characterization and experimentation.

#### 2.1.5. Characterization of synthesized Au NPs

Synthesized nanoparticles were characterized by UV-Vis spectro-photometry, transmission electron microscopy (TEM), dynamic light scattering (DLS) and zeta potential measurements. The absorbance spectra of Au NPs suspension were obtained over a wavelength range of 400 to 800 nm by using a Cary 50 Bio UV-Vis spectrophotometer (Varian, Palo Alto, CA). As described in experimental section 2.1.3, wavelengths from 200 to 800 nm indicate the presence of protein. The physical dimensions of Au NPs were determined using TEM (FEI Spirit, Hillsboro, USA) operated at 120 kV. A 400-mesh carbon-coated copper grid was glow-discharged in a vacuum evaporator (Denton, Moorestown, New Jersey) for 30 seconds to make the grid hydrophilic and attractive to particles. A drop of Au NPs stock suspension was deposited onto the grid and dried well before analysis.

To study agglomeration kinetics of Au NPs, the hydrodynamic diameter ( $D_p$ ) was measured using DLS (Malvern Instruments, Southborough, Massachusetts). Agglomeration kinetics is measured on the basis of data obtained from a time resolved mode of DLS (TR-DLS). DLS measures the light scattered from a laser passing through a colloidal solution. By analyzing the modulation of the scattered light intensity as a function of time, the hydrodynamic size of particles and particle agglomerates was determined. Larger particles diffuse more slowly than

smaller particles and the DLS instrument measures the time dependence of the scattered light to generate a correlation function that can be mathematically linked to particle size.

Agglomeration of particles depends on the surface electrical property. Surface zeta potential affects the particle interaction with other particle or molecules, therefore, it is important to know the isoelectric point where there is a zero charge on the particle surface. The zeta potential, electrophoretic mobility and conductivity was measured using a Malvern Zetasizer Nano ZS instrument. An applied voltage of 100 V was used for the NPs colloids. A minimum of three measurements were made per sample.

## **2.2. Au NP agglomeration in aqueous environment**

It is imperative to quantitatively understand the agglomeration behavior of biosynthesized Au NPs to better utilize them in applications. In the present study, agglomeration kinetics was studied in an aqueous environment, prepared by salts such as NaCl, CaCl<sub>2</sub> and MgCl<sub>2</sub>. In a series of experiments, stock solutions were prepared and filtered using a 0.1 μm syringe filter (Anatop 25, Whatman) before making further dilutions. In addition, the agglomeration was also analyzed in the presence of ethanol.

The agglomeration of Au NPs was established by measuring the hydrodynamic diameter (Dp) as a function of ionic strength, by TR-DLS. Au NPs at 10 mg/L was used for agglomeration and self-assembly studies. To provide an agglomeration medium, equal volumes (500 μL) of Au NP solution and salt solution (NaCl, CaCl<sub>2</sub> and MgCl<sub>2</sub>) were mixed into a DLS grade disposable cuvette followed by gentle vortexing. A range of salt concentrations from 0.1 M to 1 M was used. Ethanol of variable strength (25% to 100% ethanol) was mixed in Au NPs solution (500 μL Ethanol + 500 μL Au NP), Dp was measured at each 15 second up to 15 cycles.

### 2.3. Self-assembly of Au NPs in the presence of L-cysteine

L-cysteine (Sigma-Aldrich) was dissolved in deionized water in order to prepare  $6.25 \times 10^2$ ,  $1.25 \times 10^3$ ,  $2.5 \times 10^3$ ,  $5 \times 10^3$ ,  $1 \times 10^4$ , and  $2 \times 10^4$  ppm solutions. L-Cysteine and Au NPs were mixed with a 1:1 ratio. Subsequently, the solution was subjected to TR-DLS at 25°C to measure the change in hydrodynamic diameter as a function of self-assembly of Au NPs. For each sample three measurements were executed up to 120 cycles at 10 second intervals.

### 3. Results and discussion

To develop an efficient and environmentally benign protocol, Au NPs were synthesized using protein (32 mg/l) extract of tomato leaves. In this process, no other chemicals besides the precursor salt ( $\text{HAuCl}_4$ ) were used. The role of plant proteins in the bio-reduction of gold chloride and stabilization of Au NP is described through the proposed mechanistic sketch (**Figure 1**). As illustrated, the enzymatic proteins are first isolated from the plant extract. The purified enzymatic protein is mixed with  $\text{HAuCl}_4$  solution to obtain Au NPs. The purified extract contains a mixture of enzymatic proteins, some of which do not participate in the reduction reaction. These proteins may act as a natural capping agent to prevent agglomeration of the Au NPs.

The enzymatic protein extract acts as a catalyst in the reductive reaction. Thus it can be reused to react with additional precursor salt to produce more Au NPs. The concept may be used in a bio-vessel in which isolated plant enzymes can be immobilized. By adding substrate and an energy source for the enzymes, scaled-up production of Au NPs could be possible at an industrial level using plant biomass.

The as-synthesized Au NPs were characterized by UV-Vis absorption spectroscopy as a function of time to understand the biotransformation of Au particles into their nanoscale entities (**Figure 2**). Results of UV-Vis absorption spectra clearly showed a well-defined surface plasmon at 533 nm, which is in very good agreement with the reported surface plasmon resonance band of Au NPs.<sup>26</sup> The reduction of precursor salt starts at 6 h and was completed at 36 h, this reaction can be visually assessed by turning from a light yellow color (the initial color when the precursor salt was added to the plant protein extract) to a brick red color indicating Au nanoparticle formation.

To investigate the effects of protein content on gold reduction, freshly prepared precursor salt mixed with protein solution (100  $\mu\text{L}$  to 1000  $\mu\text{L}$ ) resulted in the formation of monodispersed Au NPs after 36 h, as evidenced by the color changes from 0 h to 36 h as shown in **Figure 2**. The color changes indicate the reduction of gold metal ion from  $\text{Au}^{3+}$  to  $\text{Au}^0$  and is due to the excitation of plasmon resonance in the Au NP.<sup>27</sup> This solution was stable for a prolonged time period. No agglomeration or sedimentation was observed even after 60 days. This stability of nanoparticles is possibly due to the capping proteins. However, thermal exposure, causes structural evolution, probably due thermal sensitivity of enzymatic plant proteins used for nanoparticle synthesis (**supplementary Figure 1 and Figure 2**). Results also revealed that a minimum of 250  $\mu\text{L}$  of protein solution is required to synthesize Au NPs, depending on the number of enzyme active sites available to reduce precursor salt of gold (**Figure 3**). Absorbance peaks at 260 nm are indicative of presence of certain proteins. The shorter wavelength absorbance is possibly due to low content aromatic amino acid, metal (Au) binding with protein, agglomeration and protein folding.<sup>28,29</sup>

Transmission electron microscopy analyses of synthesized Au NP revealed that the Au NPs are spherical and monodispersed (**Figure 4 A**). The role of protein in NP stabilization can be seen when the protein is removed and the NPs agglomerate (**Figure 4 B**). Similarly, Khan and Ahmad<sup>5</sup> showed that bacterial protein (13kDa) stabilized Au NPs when synthesized using a sulfite reductase enzyme. This also strongly endorses our observation that plant proteins may help to maintain the stability of NP. TEM analyses confirm that Au NPs have a physical dimension of 13-15 nm.

Electro-kinetic properties and agglomeration stability of synthetic nanoparticle in aqueous environment are required to establish the fate of the NPs and determine their applications.<sup>30-32</sup> Several factors such as, pH, salt type, ion valence, solvent types, and organic matter, are important for determining the fate and transport of NPs. Au NPs agglomeration due to NaCl, MgCl<sub>2</sub> and CaCl<sub>2</sub> salts conditions and the stability in ethanol was measured by the variation of Dp determined by time resolved DLS. Electro-kinetic measurements (**Figure 5 A**) showed that Au NPs changes polarity (either + or -) over the pH ranges between 2 and 13. Changes in electrophoretic mobility can also be explained by the variation of zeta potential (**Figure 5 B**). The zeta potential of the Au NPs drop from +36.3 to -18.5mV when the pH changes from acidic (pH 1.6) to alkaline (pH 13.3). The isoelectric point (particles with zero charge) was observed at a pH of 8.3. Unexpectedly, the conductivity of the particles decreases very rapidly (10.6 to 1.26 mS/cm) when the pH increases from 1.6 to 2.3 and remains stable until pH 10, whereas, conductivity increased further to 11.5 mS/cm when the pH was further increased to 13.3 (**Figure 5 C**).

The hydrodynamic diameter of Au NPs was observed to be greatly influenced by monovalent and divalent electrolyte solutions and ethanol (**Figure 6 A-B**). Results clearly show

that both salt and ethanol concentration are directly proportional to the hydrodynamic diameter (Dp). The diameter of Au NPs (25.6 nm) increased up to ~115 nm with the addition of electrolytes (**Figure 6 A**), whereas with increasing the ethanol concentration, Dp increased to ~570 nm (**Figure 6 B**). Liao et al.,<sup>33</sup> explained that ethanol causes dipole-dipole interaction between charged particles which results in linear agglomeration of nanoparticles. The results of monovalent and divalent electrolytes and particle agglomeration are also consistent with other engineered nanomaterials.<sup>34-36</sup> More aggressive influence of Dp by divalent ions in contrast to monovalent ions is due to a difference in charge screening as described by classical colloidal theory.<sup>37</sup>

Self-assembly of Au NPs is important to functionalize them with chemical or organic groups in order to make them functional (attach antibodies, drug molecules, fluorescent tags), and/or detectable (to establish bio-distribution, catalytic activity, or control drug delivery).<sup>38, 39</sup> Amino acids are considered as suitable agents for bio-functionalization due to the presence of –NH<sub>2</sub> or –SH groups at their terminal end, as these groups have a strong affinity for Au NPs surfaces.<sup>40</sup> Au NPs functionalized with amino acid may be used as a mimic of a protein surface, and have an important role in biomedical applications.<sup>41</sup> Thus, the amino acid, L-cysteine, containing both the functional groups was used to test whether, synthesized Au NPs could be functionalized. The self-assembly of Au NPs is directly proportional to an increasing amount of L-cysteine (**Figure 7**). DLS measurements showed Au NPs with a relatively increased hydrodynamic diameter, 100 nm and 140 nm for  $6.25 \times 10^2$  and  $2 \times 10^4$  ppm L-cysteine amino acid, respectively. The increasing size of the Au NPs indicate self-assembly of particles, although, it depends on both Au NP and available functional groups. Confirmation of Au nanoparticle functionalization as a result of L-cysteine was carried out by UV-Absorbance

spectroscopy and subsequently by fluorescent tag microscopy (**supplementary Figure 3**). Mechanistically, self-assembly of Au nanoparticles is driven by hydrogen bonds, electrostatic interactions, van der Waals forces and the dipolar interaction potential of Au NPs.<sup>42-45</sup> Surface zeta potential and polarity are the result of anisotropic association of thiol functional group of L-cysteine over gold surfaces, leading to dipole formation and Au assemblies.

#### 4. Conclusions

A simple and scalable environmentally benign approach for obtaining Au NP was demonstrated. Au NPs with mean diameter of 13-15 nm were synthesized using tomato leaf extract, and their electro-kinetic and agglomeration properties were studied. A mechanism to obtain stable protein capped nanoparticle was proposed. In addition, this process can also be exploited for scale up synthesis by immobilizing plant enzymes in a bio-vessel. Agglomeration in the presence of ionic salt and ethanol, and electro kinetic studies may also address environmental applications. It was observed that both, ionic salt and ethanol concentration is directly proportional to the hydrodynamic diameter. The diameter of Au NPs (25.6 nm) increased up to ~115 nm with the addition of electrolytes, whereas, on increasing the ethanol concentration, the size increased by ~570 nm due to agglomeration of the particles. The hydrodynamic diameter is increased due to agglomeration as a result of dipole-dipole interactions in the presence of ethanol. Induced dipole interaction is strong enough to overcome the thermal energy and electrostatic repulsion between the colloidal particles. Self-assembly of Au NPs in the presence of L-cysteine shows bio-functionalization of Au NPs, potentially having an important role in biomedical applications. The present investigation demonstrates the concept of the metal bio-reduction that may serve as a template for the production nanomaterials.

**Acknowledgments**

This work was performed in part at the Washington University in St. Louis, Nano Research Facility (NRF), and a member of the National Nanotechnology Infrastructure Network (NNIN), which is supported by the National Science Foundation under Grant No. ECS-0335765.

## References

1. M.-C. Daniel and D. Astruc, *Chem. Rev.*, 2004, **104**, 293-346.
2. H. Jans and Q. Huo, *Chem. Soc. Rev.*, 2012, **41**, 2849-2866.
3. L. Dykman and N. Khlebtsov, *Chem. Soc. Rev.*, 2012, **41**, 2256-2282.
4. P. Zhao, N. Li and D. Astruc, *Coord. Chem. Rev.*, 2013, **257**, 638-665.
5. S. A. Khan and A. Ahmad, *RSC Adv.*, 2014, **4**, 7729-7734.
6. E. C. Dreaden, A. M. Alkilany, X. Huang, C. J. Murphy and M. A. El-Sayed, *Chem. Soc. Rev.*, 2012, **41**, 2740-2779.
7. Y. Sun and Y. Xia, *Science*, 2002, **298**, 2176-2179.
8. J. Ftouni, M. Penhoat, A. Addad, E. Payen, C. Rolando and J.-S. Girardon, *Nanoscale*, 2012, **4**, 4450-4454.
9. J. A. Dahl, B. L. S. Maddux and J. E. Hutchison, *Chem. Rev.*, 2007, **107**, 2228-2269.
10. A. Malhotra, N. Sharma, Navdezda, N. Kumar, K. Dolma, D. Sharma, H. S. Nandanwar and A. R. Choudhury, *RSC Adv.*, 2014, **4**, 39484-39490.
11. K. B. Narayanan and N. Sakthivel, *Adv. Colloid Interface Sci.*, 2010, **156**, 1-13.
12. N. Durán, P. D. Marcato, M. Durán, A. Yadav, A. Gade and M. Rai, *Appl. Microbiol. Biotechnol.*, 2011, **90**, 1609-1624.
13. R. Raliya and J. Tarafdar, *Adv. Sci. Eng. Med.*, 2013, **5**, 1073-1076.
14. J. Tarafdar, S. Sharma and R. Raliya, *African J. Biotechnol.*, 2013, **12**, 219-226.
15. K. N. Thakkar, S. S. Mhatre and R. Y. Parikh, *Nanomed. Nanotechnol. Biol. Med.*, 2010, **6**, 257-262.
16. U. Shedbalkar, R. Singh, S. Wadhvani, S. Gaidhani and B. A. Chopade, *Adv. Colloid Interface Sci.*, 2014, **209**, 40-48.

17. K. J. Rao and S. Paria, *RSC Adv.*, 2014, **4**, 28645-28652.
18. P. Dasgupta, A. Bhattacharya, R. Pal, A. K. Dasgupta and S. Sengupta, *RSC Adv.*, 2015, **5**, 18429-18437.
19. N. Basavegowda, A. Idhayadhulla and Y. R. Lee, *Ind. Crop. Prod.*, 2014, **52**, 745-751.
20. M. F. Zayed and W. H. Eisa, *Spectrochim Acta A Mol. Biomol. Spectrosc.*, 2014, **121**, 238-244.
21. S. Iravani, *Green Chem.*, 2011, **13**, 2638-2650.
22. G. Barman, S. Maiti and J. Laha, *Nanoscale Res. Lett.*, 2013, **8**, 1-9.
23. A. A. Keller, H. Wang, D. Zhou, H. S. Lenihan, G. Cherr, B. J. Cardinale, R. Miller and Z. Ji, *Environ. Sci. Technol.*, 2010, **44**, 1962-1967.
24. W. N. Wang, J. C. Tarafdar and P. Biswas, *J. Nanopart. Res.*, 2013, **15**, 151417.
25. D. Shenoy, W. Fu, J. Li, C. Crasto, G. Jones, C. DiMarzio, S. Sridhar and M. Amiji, *Int J Nanomedicine*, 2006, **1**, 51.
26. R. Sardar, T. B. Heap and J. S. Shumaker-Parry, *J. Am. Chem. Soc.*, 2007, **129**, 5356-5357.
27. M. Wyatt, C. Johnston and N. Magarvey, *J. Nanopart. Res.*, 2014, **16**, 1-7.
28. C. F. Bohren and D. R. Huffman, *Absorption and scattering of light by small particles*, John Wiley & Sons, 2008.
29. V. F. Kalb Jr and R. W. Bernlohr, *Anal. Biochem.*, 1977, **82**, 362-371.
30. A. Albanese and W. C. W. Chan, *ACS Nano*, 2011, **5**, 5478-5489.
31. D. Bouchard, W. Zhang, T. Powell and U. s. Rattanaudompol, *Environ. Sci. Technol.*, 2012, **46**, 4458-4465.

32. I. Chowdhury, M. C. Duch, N. D. Mansukhani, M. C. Hersam and D. Bouchard, *Environ. Sci. Technol.*, 2013, **47**, 6288-6296.
33. J. Liao, Y. Zhang, W. Yu, L. Xu, C. Ge, J. Liu and N. Gu, *Colloids Surf. Physicochem. Eng. Aspects*, 2003, **223**, 177-183.
34. V. Chegel, O. Rachkov, A. Lopatynskiy, S. Ishihara, I. Yanchuk, Y. Nemoto, J. P. Hill and K. Ariga, *J. Phys. Chem. C*, 2011, **116**, 2683-2690.
35. L. Wu, L. Liu, B. Gao, R. Muñoz-Carpena, M. Zhang, H. Chen, Z. Zhou and H. Wang, *Langmuir*, 2013, **29**, 15174-15181.
36. J. K. Jiang, G. Oberdorster and P. Biswas, *J. Nanopart. Res.*, 2009, **11**, 77-89.
37. M. Elimelech, X. Jia, J. Gregory and R. Williams, *Particle deposition & aggregation: measurement, modelling and simulation*, Butterworth-Heinemann, 1998.
38. R. Ren, S. Li, J. Li, J. Ma, H. Liu and J. Ma, *Catalysis Science & Technology*, 2015, **5**, 2149-2156.
39. V. Liljeström, J. Mikkilä and M. A. Kostianen, *Nat Commun*, 2014, **5**, 1-9.
40. S. Aryal, R. BKC, N. Dharmaraj, N. Bhattarai, C. H. Kim and H. Y. Kim, *Spectrochim Acta A Mol. Biomol. Spectrosc.*, 2006, **63**, 160-163.
41. N. Wangoo, S. Kaur, M. Bajaj, D. Jain and R. K. Sharma, *Nanotechnology*, 2014, **25**, 435608.
42. M. Yang, G. Chen, Y. Zhao, G. Silber, Y. Wang, S. Xing, Y. Han and H. Chen, *Phys Chem Chem Phys*, 2010, **12**, 11850-11860.
43. H. Zhang and D. Wang, *Angew. Chem.*, 2008, **120**, 4048-4051.
44. Y. Min, M. Akbulut, K. Kristiansen, Y. Golan and J. Israelachvili, *Nat. Mater.*, 2008, **7**, 527-538.

45. F. Wang, X. Liu, C.-H. Lu and I. Willner, *ACS Nano*, 2013, **7**, 7278-7286.

## List of Figures

- Figure 1.** Proposed mechanism for the bio-inspired green approach for Au NPs synthesis. (i) Tomato plants leaves collected from 14 days old plant, through which enzymatic proteins were extracted (ii) Enzymatic proteins were mixed with precursor salt solution to synthesize Au NPs. Enzymes donate three electron which results in Au nanoparticles were synthesis from precursor salt solution (AuCl<sub>4</sub><sup>-</sup>).
- Figure 2.** UV-Vis absorption spectra of Au NPs as a function of incubation time. Inset shows color changes in solution with the bio-reduction of Au<sup>+3</sup> to Au<sup>0</sup>.
- Figure 3.** UV-Vis spectra of different protein concentration used for Au NPs synthesis after 36 h. Inset spectrum shows corresponding Au NPs peak at 533 nm.
- Figure 4.** TEM micrograph of Au NPs (a) Protein capped stable and monodisperse nanoparticle (b) Naked (without protein capped) Au NPs.
- Figure 5.** Electrokinetic characterization of Au NPs as a function of pH (A) Electrophoretic mobility (B) Zeta potential (C) Conductivity.
- Figure 6.** Change in hydrodynamic diameter, D<sub>p</sub> due to agglomeration for (A) Different concentrations of electrolytes: NaCl, MgCl<sub>2</sub>, CaCl<sub>2</sub> (B) Different times at six different ethanol concentrations (25, 50, 75, 80, 90 and 100%).
- Figure 7.** Change in hydrodynamic diameter (D<sub>p</sub>) of biosynthesized Au NPs with time for 6 different concentrations of cysteine.

**List of Tables**

**Table 1.** Experimental plan for environmentally benign bioinspired approach for Au NPs synthesis

**Table 1.** Experimental plan for environmentally benign bioinspired approach for Au nanoparticle synthesis

Sr. No.	Experiment	Objective	Characterization or Analyses	Notes
I	<p><b>Synthesis of Au NPs</b></p> <p><b>a.</b> Isolation and quantification of plant protein</p> <p><b>b.</b> time dependent investigation for Au NPs synthesis</p> <p><b>c.</b> Effect of protein concentration on Au NPs formation</p> <p><b>d.</b> Purification of synthesized nanoparticles</p>	Green synthesis	<p><b>i.</b> UV-Vis spectrophotometer, transmission electron microscopy (TEM) and dynamic light scattering (DLS)</p> <p><b>ii.</b> Electrokinetic characterization</p>	Figure 2 to 5 (Detail of synthesis procedure are described in Figure 1)
II	Au NPs agglomeration in aqueous environment	Stability and fate studies	Time Resolved-Dynamic light scattering (TR-DLS)	Figure 6 (In response to ionic salt and ethanol-water environment)
III	Self-assembly of Au NPs	Potential to functionalize with other agents	TR-DLS	Figure 7 (In the presence of L-cysteine)

## Figures

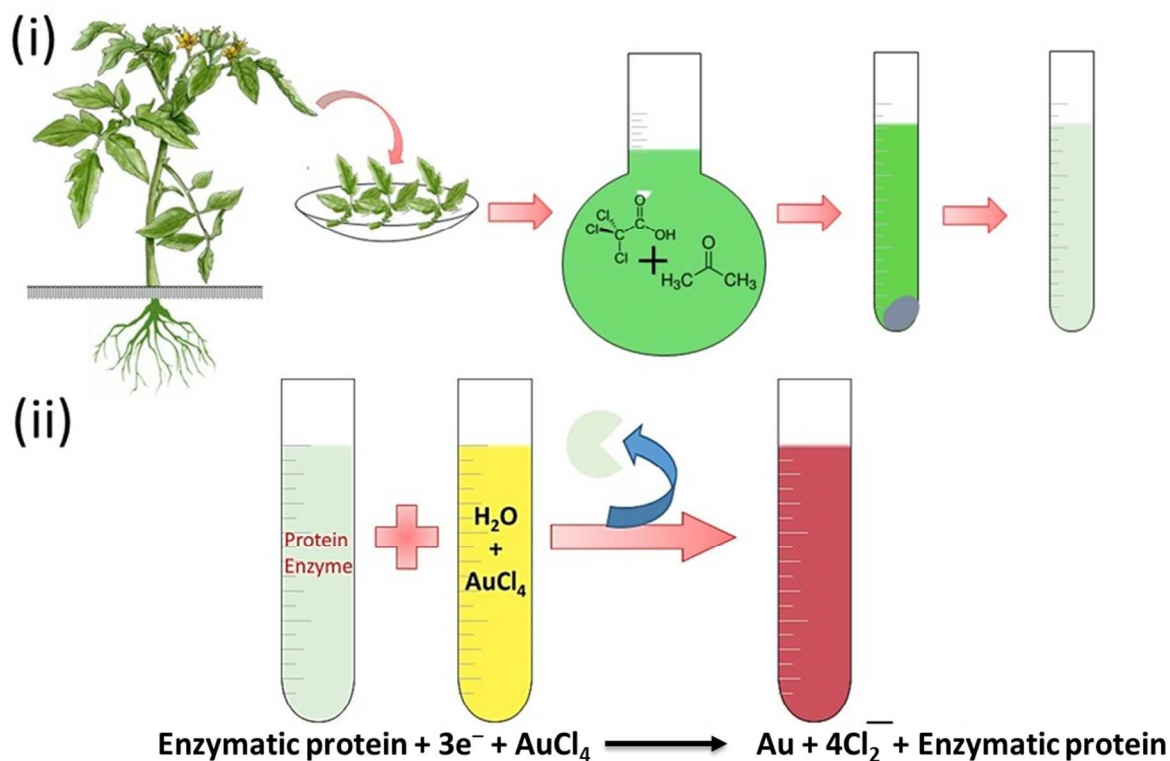


**Figure 1.** Proposed mechanism for the bio-inspired green approach for Au NPs synthesis. (i) Tomato plants leaves collected from 14 days old plant, through which enzymatic proteins were extracted (ii) Enzymatic proteins were mixed with precursor salt solution to synthesize Au NPs. As the reaction showed, Enzymes donate three electrons which results in Au NPs were synthesis from precursor salt solution (AuCl<sub>4</sub>).

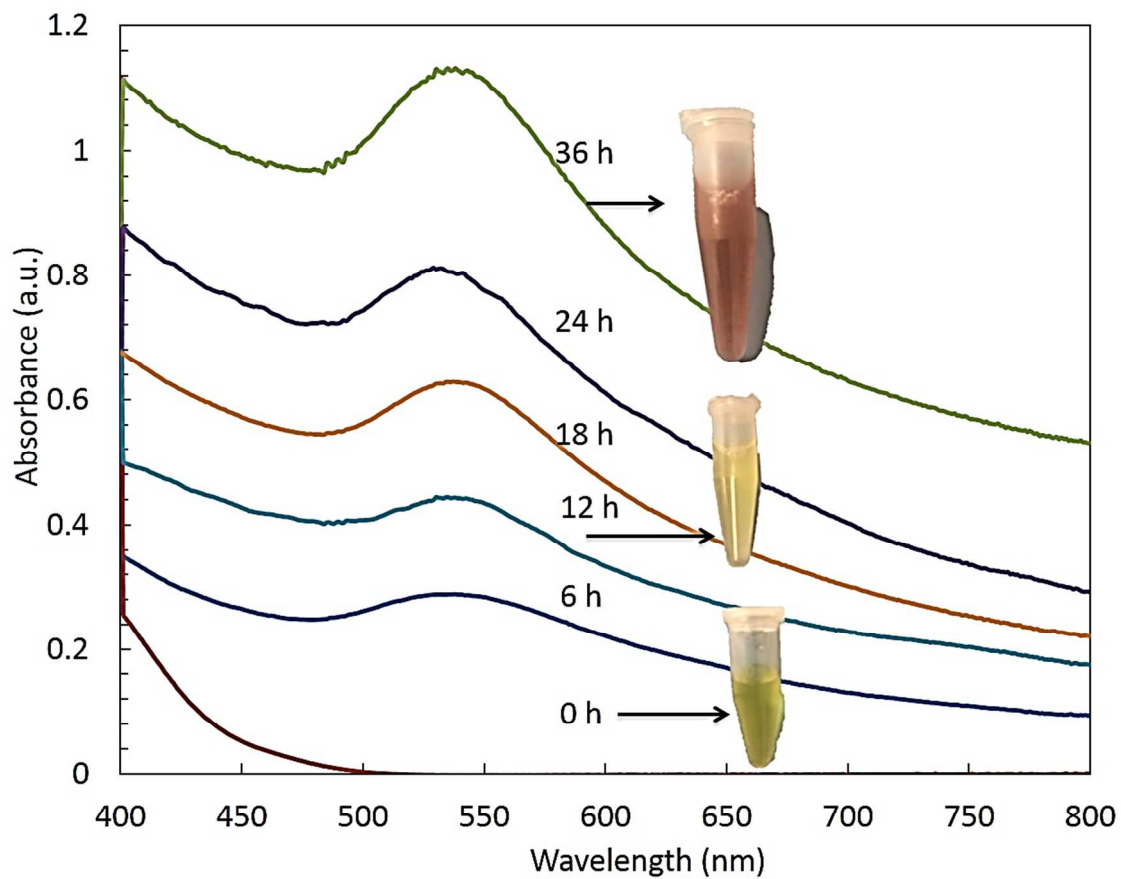


**Figure 2.** UV-Vis absorption spectra of Au NPs for different incubation times. Inset shows color changes in solution with the bio-reduction of  $\text{Au}^{+3}$  to  $\text{Au}^0$ .

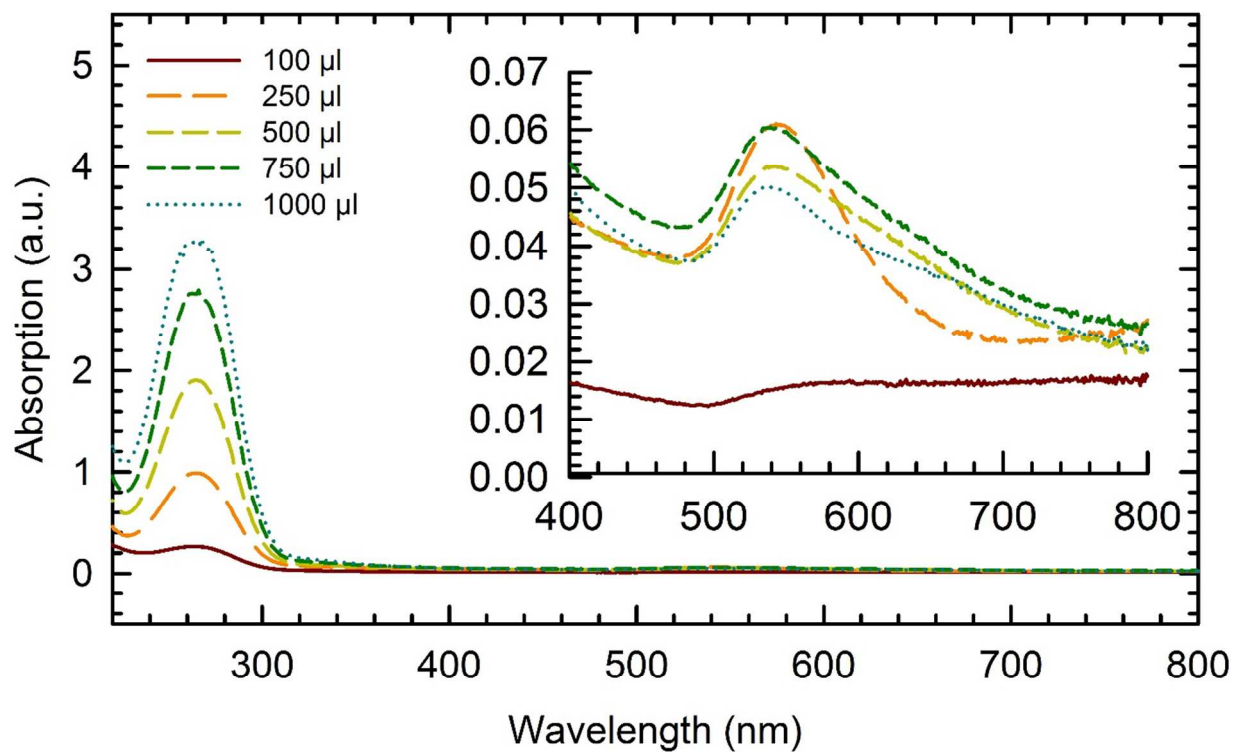


**Figure 3.** UV-Vis spectra of different protein concentration used for Au NP synthesis after 36 h.

Inset spectrum shows corresponding Au NPs peak at 533 nm

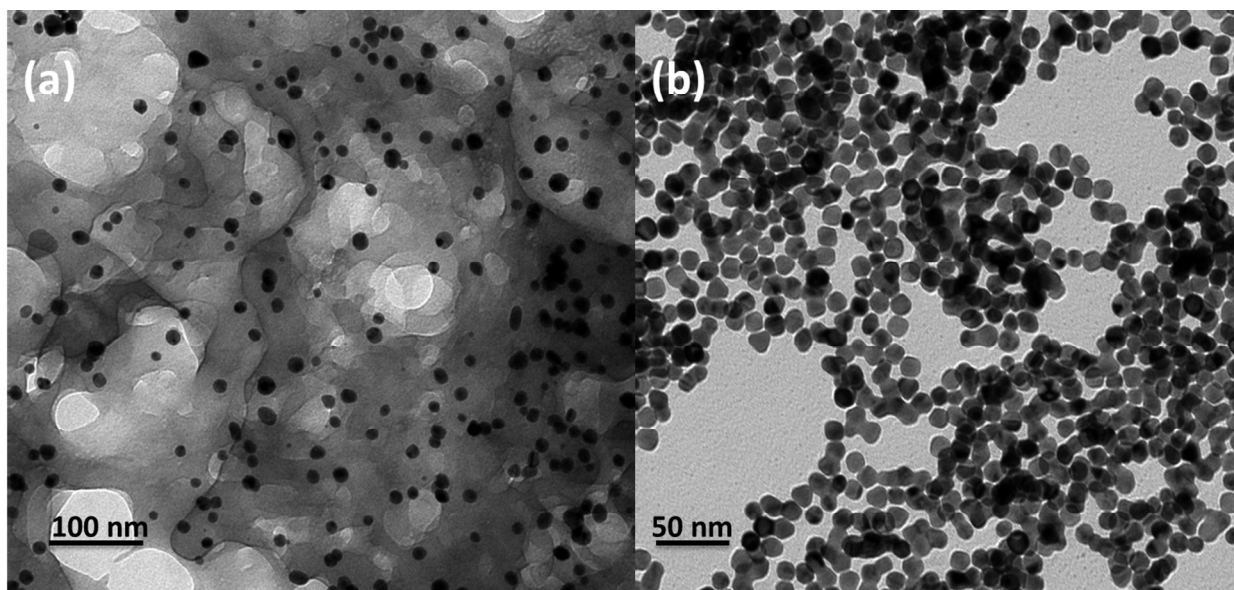


**Figure 4.** TEM micrograph of Au NPs (a) Protein capped stable and monodisperse nanoparticle  
(b) Naked (without protein capped) Au NPs

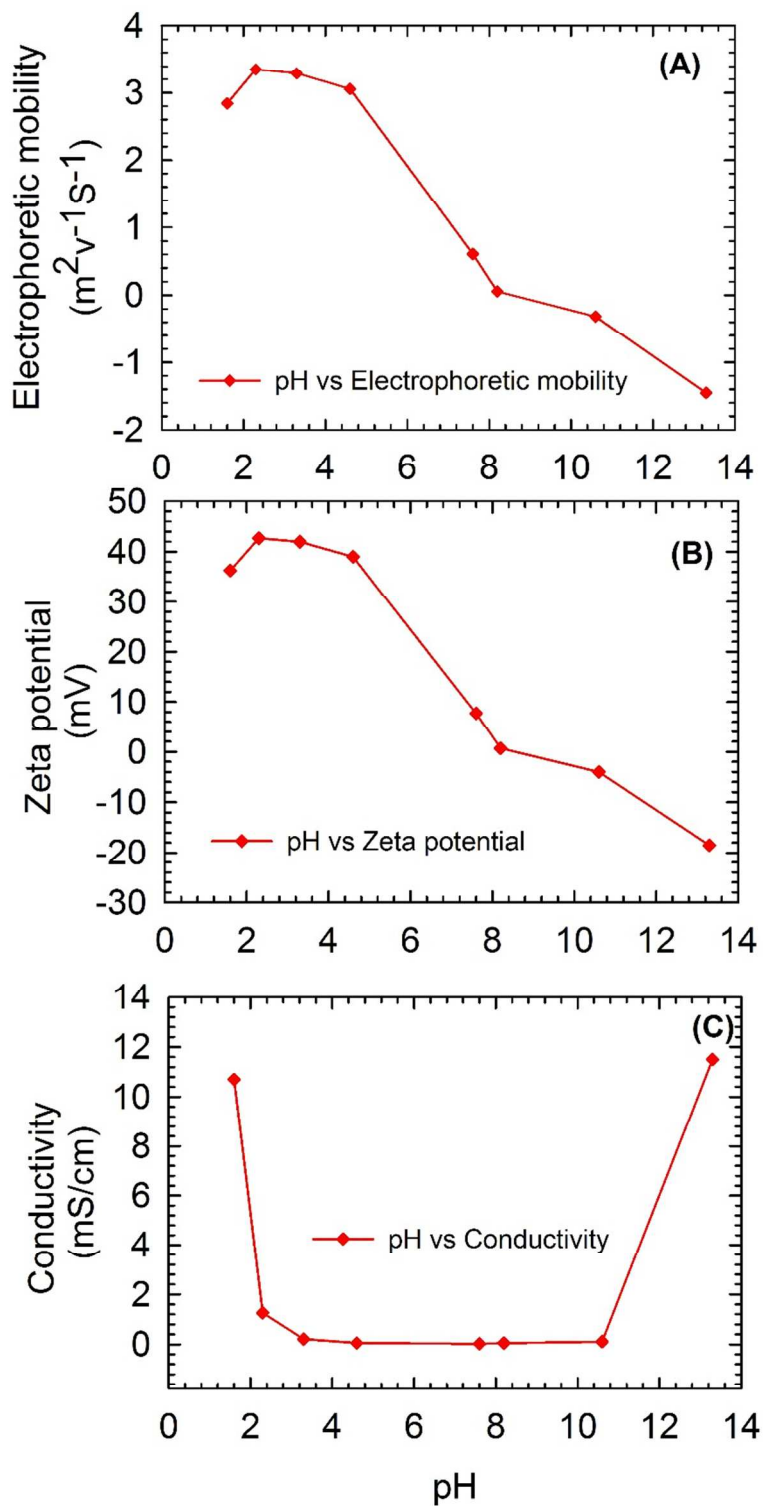


**Figure 5.** Electrokinetic characterization of Au NPs as a function of pH (A) Electrophoretic mobility (B) Zeta potential (C) Conductivity

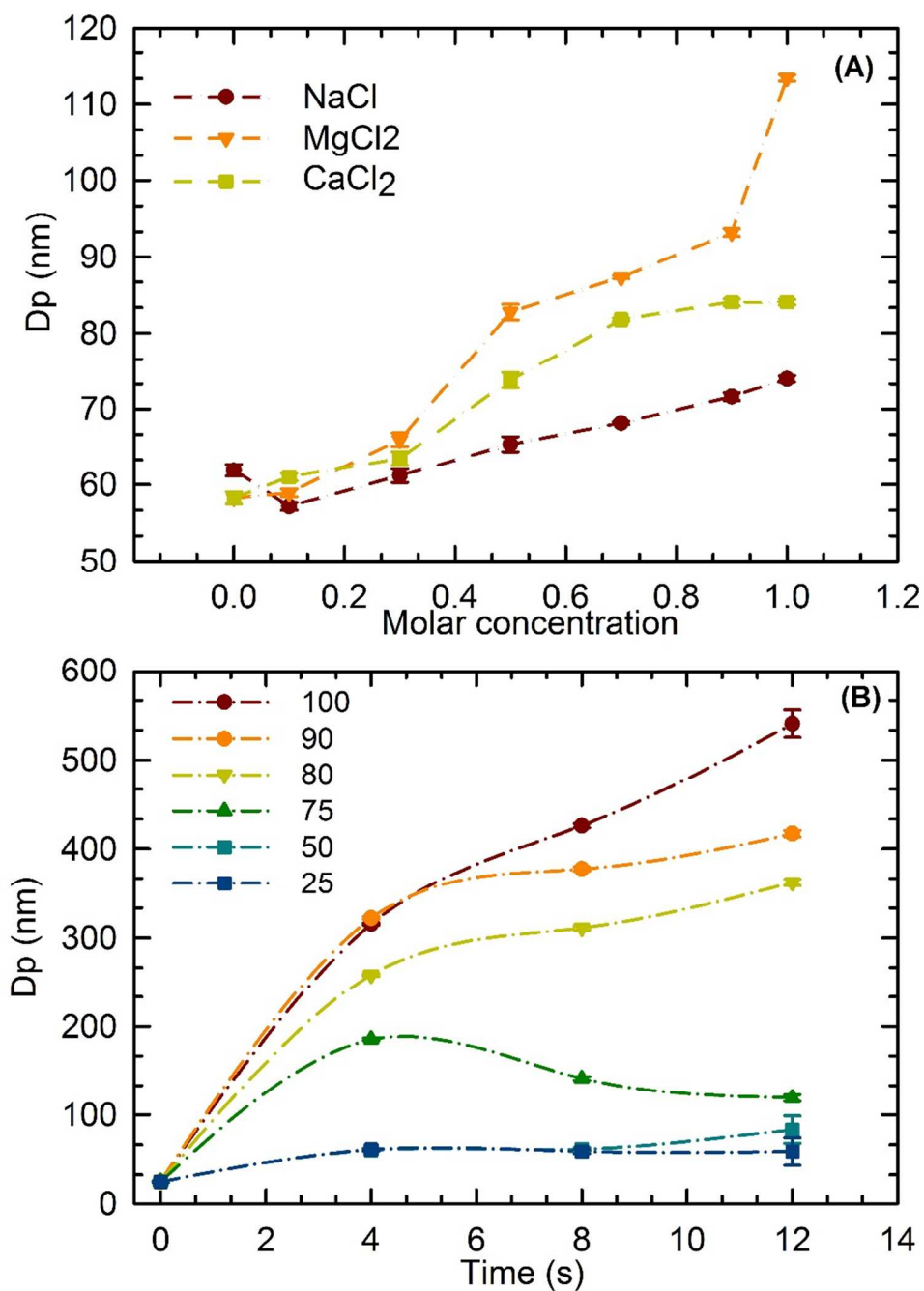


**Figure 6.** Change in hydrodynamic diameter, Dp due to agglomeration for (A) Different concentrations of electrolytes: NaCl, MgCl<sub>2</sub>, CaCl<sub>2</sub> (B) Different times at six different ethanol concentrations (25, 50, 75, 80, 90 and 100%).

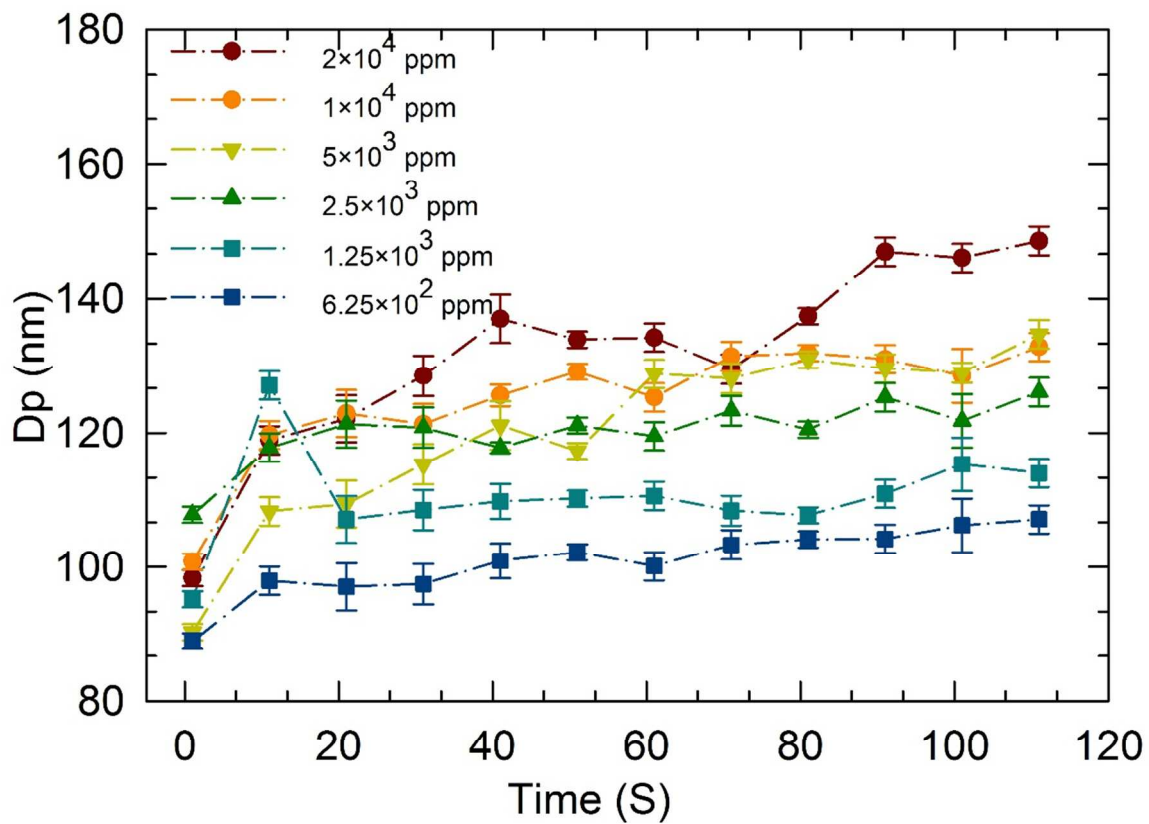


**Figure 7.** Change in hydrodynamic diameter (Dp) of biosynthesized Au NPs with time for 6 different concentrations of cysteine.